

Exceptional aggressiveness of cerebral cavernous malformation disease associated with *PDCD10* mutations

Robert Shenkar, PhD¹, Changbin Shi, MD, PhD¹, Tania Rebeiz, MD², Rebecca A. Stockton, PhD³, David A. McDonald, PhD^{4,5}, Abdul Ghani Mikati, MD¹, Lingjiao Zhang, MS¹, Cecilia Austin, BS¹, Amy L. Akers, PhD⁶, Carol J. Gallione, BA⁴, Autumn Rorrer, BA⁴, Murat Gunel, MD⁷, Wang Min, PhD⁸, Jorge Marcondes de Souza, MD, PhD⁹, Connie Lee, PsyD⁶, Douglas A. Marchuk, PhD⁴ and Issam A. Awad, MD, MSc^{1,2}

Purpose: The phenotypic manifestations of cerebral cavernous malformation disease caused by rare *PDCD10* mutations have not been systematically examined, and a mechanistic link to Rho kinase-mediated hyperpermeability, a potential therapeutic target, has not been established.

Methods: We analyzed *PDCD10* small interfering RNA-treated endothelial cells for stress fibers, Rho kinase activity, and permeability. Rho kinase activity was assessed in cerebral cavernous malformation lesions. Brain permeability and cerebral cavernous malformation lesion burden were quantified, and clinical manifestations were assessed in prospectively enrolled subjects with *PDCD10* mutations.

Results: We determined that *PDCD10* protein suppresses endothelial stress fibers, Rho kinase activity, and permeability in vitro. *Pdcd10* heterozygous mice have greater lesion burden than other *Ccm* genotypes. We demonstrated robust Rho kinase activity in murine and

human cerebral cavernous malformation vasculature and increased brain vascular permeability in humans with *PDCD10* mutation. Clinical phenotype is exceptionally aggressive compared with the more common *KRIT1* and *CCM2* familial and sporadic cerebral cavernous malformation, with greater lesion burden and more frequent hemorrhages earlier in life. We first report other phenotypic features, including scoliosis, cognitive disability, and skin lesions, unrelated to lesion burden or bleeding.

Conclusion: These findings define a unique cerebral cavernous malformation disease with exceptional aggressiveness, and they inform preclinical therapeutic testing, clinical counseling, and the design of trials.

Genet Med advance online publication 14 August 2014

Key Words: *CCM3*; cerebral cavernous malformation; *PDCD10*; Rho kinase; vascular malformations

INTRODUCTION

Cerebral cavernous malformations (CCMs) are clusters of grossly dilated brittle capillaries that predispose patients to a lifetime risk of hemorrhagic stroke, epilepsy, and other sequelae.¹ Familial forms account for about a third of cases and involve autosomal dominant inheritance at one of three gene loci.² No current treatment for CCM exists, except highly invasive surgical procedures for resecting symptomatic lesions. Despite promising pharmacotherapeutic targets,^{3–5} progress to clinical trials has been hindered by the relatively benign manifestations of CCM disease in general, a low rate of new lesion development, and the unpredictability of serious clinical events.^{6–8}

Few studies have examined any special features of the rarest cases with programmed cell death 10 (*PDCD10*) mutation (also known as the *CCM3* locus), constituting <15% of probands genotyped by sequential mutation screening and <2% of

CCM cases at large. Our group and others have suggested different disease aggressiveness with various CCM genotypes,^{9–11} and bleeding at a young age and meningiomas were recently associated with *PDCD10* cases.¹² There has, however, been no systematic assessment of lesion burden, hemorrhage risks per lesion and per patient, or other comprehensive phenotypic survey in probands with this mutation. The potential link of Rho kinase (ROCK) activity to the loss of *PDCD10* protein had been suggested previously,^{13,14} but it has not been linked to vascular hyperpermeability as with other CCM genotypes.¹⁵ ROCK activity has not been previously examined in vascular lesions from these patients, nor has their brain permeability in vivo. Other reports have suggested that *PDCD10* mutations might cause CCM via distinct Rho-independent mechanisms.^{16–20}

Herein we confirm that *PDCD10* loss is associated with increased ROCK activity, stress fiber induction, and

The first two authors are co-first authors, and the last two authors are co-senior authors.

¹Neurovascular Surgery Program, Section of Neurosurgery, The University of Chicago Medicine, Chicago, Illinois, USA; ²Department of Neurology, The University of Chicago Medicine, Chicago, Illinois, USA; ³Department of Pediatrics, University of California, Los Angeles, Torrance, California, USA; ⁴Department of Molecular Genetics and Microbiology, Duke University, Durham, North Carolina, USA; ⁵Center for Science, Math and Technology Education, North Carolina Central University, Durham, North Carolina, USA; ⁶Angioma Alliance, Norfolk, Virginia, USA; ⁷Department of Neurosurgery and Neurobiology, Yale University, New Haven, Connecticut, USA; ⁸Department of Pathology, Yale University, New Haven, Connecticut, USA; ⁹Department of Neurosurgery, School of Medicine, Federal University of Rio de Janeiro, Rio de Janeiro, Brazil. Correspondence: Issam A. Awad (iawad@uchicago.edu)

Submitted 6 April 2014; accepted 23 June 2014; advance online publication 14 August 2014. doi:[10.1038/gim.2014.97](https://doi.org/10.1038/gim.2014.97)

endothelial permeability in vitro, which are rescued by ROCK inhibition. We also demonstrate ROCK activity in CCM vasculature in mice and humans, defining a mechanistic link and a potential therapeutic target. We show that *Pdcd10* and *PDCD10* mutations result in significantly greater lesion burden in mice and humans, respectively, than other CCM disease and more severe clinical manifestations, and we document several novel clinical associations. We report that the brain of *PDCD10* patients manifests vascular hyperpermeability, confirming the expected impact of ROCK activity in vivo. The exceptionally high rates of lesion formation and symptomatic hemorrhage motivate novel hypotheses for mechanistic studies and provide an opportunity to focus

preclinical optimization and early therapeutic trials on this small but seriously affected subgroup of CCM cases.

MATERIALS AND METHODS

Details for human subjects, cell culture, the *Pdcd10*^{+/-}*Trp53*^{-/-} heterozygous murine model, genetic testing in subjects, transfection, immunofluorescence, western blotting, RhoA activation assay, permeability assay in vitro, sample preparation and histology, immunohistochemistry, lesion burden and in vivo brain permeability in humans, lesion burden and clinical features, statistical methods, and control comparisons are provided in **Supplementary Materials and Methods** online. Methods for the assessment of endothelial barrier function

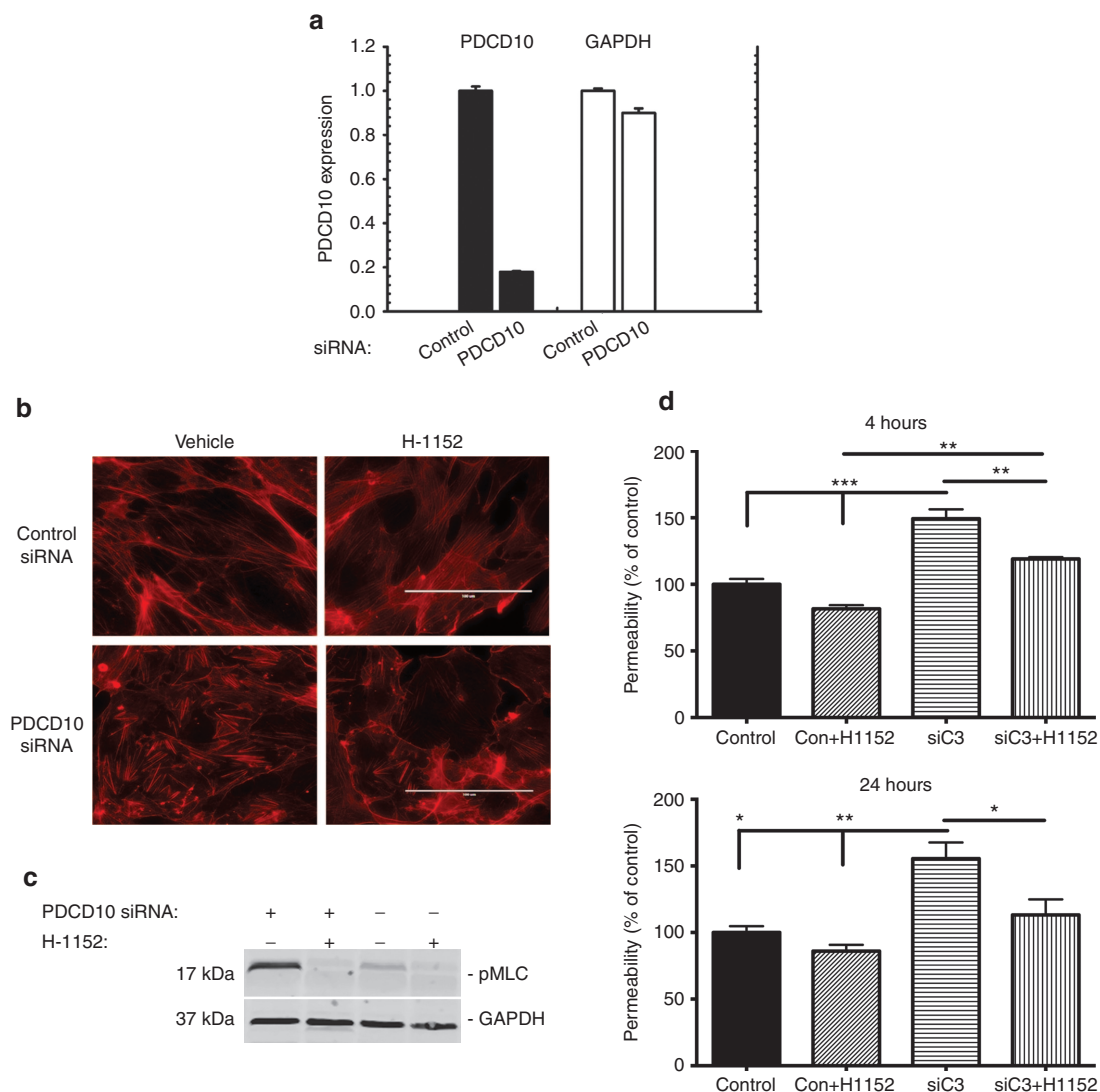


Figure 1 *PDCD10* suppresses stress fibers, Rho kinase (ROCK) activity, and permeability in vitro. Human umbilical vein endothelial cells (HUVECs) were treated with control or *PDCD10* small interfering RNA (siRNA). **(a)** *PDCD10* gene expression is reduced by 80% by *PDCD10* siRNA in HUVECs compared with those treated with control siRNA. Data bars are means \pm SE. **(b)** Increase in f-actin stress fibers by *PDCD10* depletion is blunted by the ROCK inhibitor H-1152. Bar = 100 μ m. **(c)** Increased phosphorylated myosin light chain activity by *PDCD10* depletion is reversed by H-1152. **(d)** *PDCD10* depletion over 4 and 24 hours increases monolayer permeability in transwell assays. H-1152 treatment reverses this increase, implying that *PDCD10* inhibits ROCK-mediated monolayer leak. Data bars are means \pm SE of $n = 3$. Analysis by analysis of variance indicates * $P < 0.05$, ** $P < 0.01$, *** $P < 0.001$.

in vitro,¹⁵ preparation of murine brain sections,³ and ROCK activity assays^{3,15} have been described previously.

RESULTS

PDCD10 inhibits ROCK and maintains endothelial barrier function

Knockdown efficacy was shown by an ~80% reduction in *PDCD10* message in human umbilical vein endothelial cells transfected with *PDCD10* small interfering RNA (siRNA) (Figure 1a). Control and *PDCD10* siRNA-treated human umbilical vein endothelial cells were stained for f-actin to show the extent of stress fiber content (Figure 1b). Stress fiber content was increased with *PDCD10* depletion. This increase was reversed by the ROCK inhibitor H-1152. These effects were confirmed in human brain microvascular cells when *KRIT1*, *CCM2*, or *PDCD10* siRNA was used (Supplementary Figure S1 online). A consequence of ROCK activation is phosphorylation of myosin light chain (MLC). To monitor ROCK activity, control and *PDCD10* siRNA-treated human umbilical vein endothelial cells were stained for phosphorylated MLC after western blotting (Figure 1c). *PDCD10* depletion increased ROCK activity, which was suppressed by H-1152. These effects were confirmed in human brain microvascular cells, whereas total MLC levels were not affected by *PDCD10* depletion or H-1152 (Supplementary Figure S2 online). Rho-guanosine triphosphate activity was increased after *KRIT1*, *CCM2*, or *PDCD10* knockdown (Supplementary Figure S3 online). Stability of endothelial cell junctions was measured by permeability of control and *PDCD10* siRNA-treated human umbilical vein endothelial cell monolayers (Figure 1d). Upon *PDCD10* depletion the monolayers became more permeable. This increased leakage was reversed by H-1152, indicating rescue of the hyperpermeable endothelial phenotype by ROCK inhibition despite *PDCD10* loss.

Pdcd10 heterozygous mouse models have more numerous and larger CCM lesions

Total lesion burden per mouse was significantly greater ($P < 0.001$) when comparing 15 *Pdcd10*^{+/-} sensitized animals in the *Trp53*^{-/-} background with 53 mice with other heterozygous CCM genotypes (*Krit1*^{+/-} or *Ccm2*^{+/-}) in the same backgrounds (Supplementary Table S1 online). The sensitized *Pdcd10*^{+/-}*Trp53*^{-/-} model had over sevenfold more prevalent CCM lesions than similarly sensitized models of *Krit1*^{+/-}*Trp53*^{-/-} or *Ccm2*^{+/-}*Trp53*^{-/-} genotypes and also a greater burden of mature stage 2 lesions.

Even nonsensitized *Pdcd10*^{+/-} mice (without *Trp53* loss) manifested typical CCM lesions (mean 1.6 lesions/mouse); no such lesions were documented in nonsensitized heterozygotes of other CCM genotypes ($P < 0.001$). The mean area for the stage 2 lesions was larger in the *Pdcd10*^{+/-}*Trp53*^{-/-} model (0.94 mm² per lesion) than in other sensitized genotypes (0.34 mm²/lesion; $P < 0.01$). Based on these mouse models, it is clear that heterozygous loss of *Pdcd10*, with or without genetic sensitization, leads to a more severe and penetrant CCM phenotype than loss of either *Krit1* or *Ccm2*.

Cerebral endothelial cell ROCK activity is present in *Pdcd10* heterozygous mice

ROCK activity was present in CCM lesions and in background capillaries in both sensitized and nonsensitized *Pdcd10* models as assessed by staining of phosphorylated MLC and phosphorylated myosin-binding substrate (Supplementary Figure S4 online), whereas no such activity is seen in capillaries of wild-type control mice.²¹ The prevalence of phosphorylated MLC immunopositive caverns was the same in CCM lesions regardless of sensitized or nonsensitized background (95.4% of 1,111 caverns counted in 79 lesions present in 5 *Pdcd10*^{+/-}*Trp53*^{-/-} mice versus 96.5% of 142 caverns counted in 23 lesions in 11 nonsensitized *Pdcd10*^{+/-} mice), indicating that ROCK activity in CCM lesions is related to the *Pdcd10* mutations and not the background sensitizer. These results complement our in vitro experiments by demonstrating the effect of *Pdcd10* mutations on ROCK activity in vivo.

Cerebral endothelial ROCK activity in human CCM lesions

We demonstrated ROCK activity in human *PDCD10* CCM lesions, as in murine lesions. Human *PDCD10* CCM lesions had twice as many caverns with ROCK activity than human *KRIT1*, *CCM2*, and sporadic CCM lesions ($P < 0.05$; Figure 2).

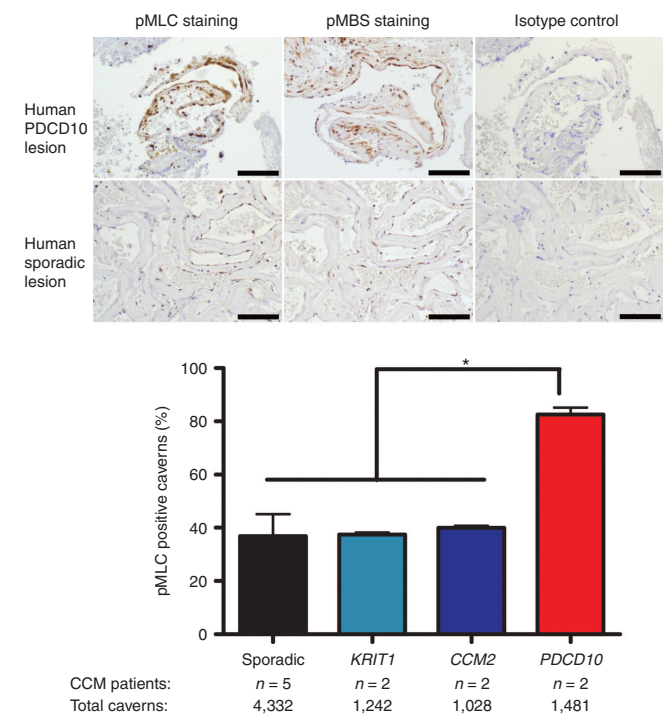


Figure 2 Rho kinase (ROCK) activity in cerebral cavernous malformation (CCM) lesions in human subjects. There is greater ROCK activity in human *PDCD10* CCM lesions than in human sporadic lesions, as shown by brown phosphorylated myosin light chain (pMLC) and phosphorylated myosin binding substrate staining. The histogram shows that twice as many caverns have at least one endothelial cell stained with pMLC in human *PDCD10* CCM lesions than in human *KRIT1*, *CCM2*, and sporadic lesions ($*P < 0.05$). Data bars are means \pm SE. Bars = 100 μ m.

Table 1 *PDCD10* proband mutations all lead to loss-of-function alleles

Family	Mutation	Effect
1	c.180delA, p.60fsX64	Nonsense
2	c.474+5G>A	Splicing
3	c.474+1G>A	Splicing
4	c.322C>T; p.Arg108Stop	Nonsense
5	c.608T>G; p.Leu203Stop	Nonsense
6	c.474+5G>A	Splicing
7	c.474+5 G>A	Splicing
8	c.124C>T; p.Gln42Stop	Nonsense
9	c.474+1G>A	Splicing
10	c.131T>C; p.Leu44Pro	Missense
11	c.501delT, p.167fsX168	Nonsense
12	c.103C>T; p.Arg35Stop	Nonsense
13	c.475-2A>G	Splicing

Spectrum of mutations in *PDCD10* in humans and prevalence of spontaneous mutations

The allelic series of *PDCD10* mutations is cataloged in [Table 1](#). All mutations are predicted to lead to a loss-of-function allele. In 12 of 13 probands, mutations included nonsense and splice site–altering mutations. Proband 12 carried a missense mutation: c.131T>C;p.Leu44Pro. This helix-breaking mutation is predicted to result in loss of function by disrupting helix α C of the *PDCD10* protein, thereby inhibiting both *PDCD10* homodimerization and binding to the germinal center kinase III kinases.²² Sixteen of the 18 patients underwent parental screening for their index *PDCD10* mutation. Seven of the 16 cases with parental screening (44%) harbored a spontaneous de novo mutation not inherited from either parent.

Early-onset hemorrhage and high risk of recurrent bleeds in humans

The mean age at presentation of the first clinical symptom was 12.6 years (range 0.25–52). Symptomatic CCM bleed was the most common presenting event, affecting 10 of 18 subjects (56%), who suffered 37 overt hemorrhages. Estimated incidence of hemorrhage was 7.9% (confidence interval (CI): 5.6–11) per patient per year based on exposure risk since birth and 20% (CI: 14–28) per patient per year based on risk since onset of first symptom. The risk of recurrent bleed after a first bleed was 24% (CI: 16–35) per patient per year. There were significant associations between the annual bleed rate and a younger age at first-symptom onset, at first bleed, and at diagnosis ($P < 0.001$ for all) but no significant difference between the sexes. Life tables of hemorrhage risk from birth, from first symptom, and from first bleed are presented in [Figure 3a,b](#).

The first overt hemorrhage occurred most often in the first decade of life (mean age: 5.9 years; range: 0.33–12 years). This is significantly earlier than the age at first bleed in *KRIT1* and *CCM2* familial cases evaluated in our clinic (mean age: 30 years; range: 1–52 years; $P < 0.05$) and in the clinical data set of the Angioma Alliance DNA/Tissue Bank

(mean age: 32 years; range: 3–55 years; $P < 0.001$; [Figure 3c](#) and [Supplementary Figure S5](#) online).

Exceptional lesion burden in humans, as in mice, with low bleeding rate per lesion

Lesion burden on susceptibility weighted imaging (SWI) was exceptionally high: 33% of *PDCD10* cases harbored >100 lesions and 78% harbored >20 lesions. The mean number of lesions per patient on T2-weighted magnetic resonance imaging (MRI) scan was 31.33 (CI: 20.64–47.57) in *PDCD10* cases, significantly greater than the mean lesion count of 5.25 (CI: 2.38–11.59) in familial *KRIT1* and *CCM2* cases ($P < 0.001$). When adjusted for age, the SWI lesion burden was also significantly greater in the *PDCD10* cohort than in control familial cases with *KRIT1* or *CCM2* mutations (2.03 SWI lesions/year of life in *PDCD10* versus 1.08 in *KRIT1* and *CCM2* cases; $P < 0.01$). *PDCD10* patients form 2.36 new lesions on T2-weighted MRI per year of follow-up, compared with 0.30 new lesions per year of follow-up in *KRIT1* cases ($P = 0.002$). Among 9 cases that underwent 19 prospective repeated MRI scans with comparable technique, there were 2.7 (CI: 1.8–3.9) new SWI lesions per patient per year of follow-up. An MRI scan from one such case with exceptionally high SWI lesion burden is shown in [Figure 3d](#).

Bleeding rate per lesion per year after first-symptom onset was 0.3% (CI: 0.2–0.4), similar to that previously reported in other CCM genotypes.^{6–8,23–25} The rebleeding rate per lesion after a first bleed from any lesion was only slightly higher at 0.4% (CI: 0.23–0.52). This suggests that the high bleeding rate in *PDCD10* subjects is due to the exceptional lesion burden rather than any particularly higher hemorrhagic propensity of individual CCM lesions. CCM lesions in SWI scans formed at a rate of 2.03 lesions (CI: 1.89–2.16) per patient per year of life.

Increased brain permeability in humans

Using dynamic contrast-enhanced quantitative perfusion ([Supplementary Figure S6](#) online), we found that patients with *PDCD10* mutations exhibited increased permeability in white matter far from the lesions compared to sporadic CCM cases without germline mutations ($P < 0.05$). This finding also was observed in other familial cases (unpublished data). Lesional permeability in *PDCD10* cases was higher than in *KRIT1* cases. This confirms a functional impact of ROCK activity associated with *PDCD10* mutations in vivo.

Other clinical features of *PDCD10* mutation

[Figure 4](#) illustrates each symptomatic bleed noted during the life span of each subject, groups the cases by their respective proband, and presents relevant information about each subject's lesion burden and clinical associations.

Skin lesions were noted in five cases (28%). Two patients had café-au-lait lesions, one had a scalp hemangioma, and two had cutaneous cavernous malformations (both confirmed by biopsy). Scoliosis was documented in seven cases (39%). Three of these patients had spinal fusion due to severe scoliosis. Of

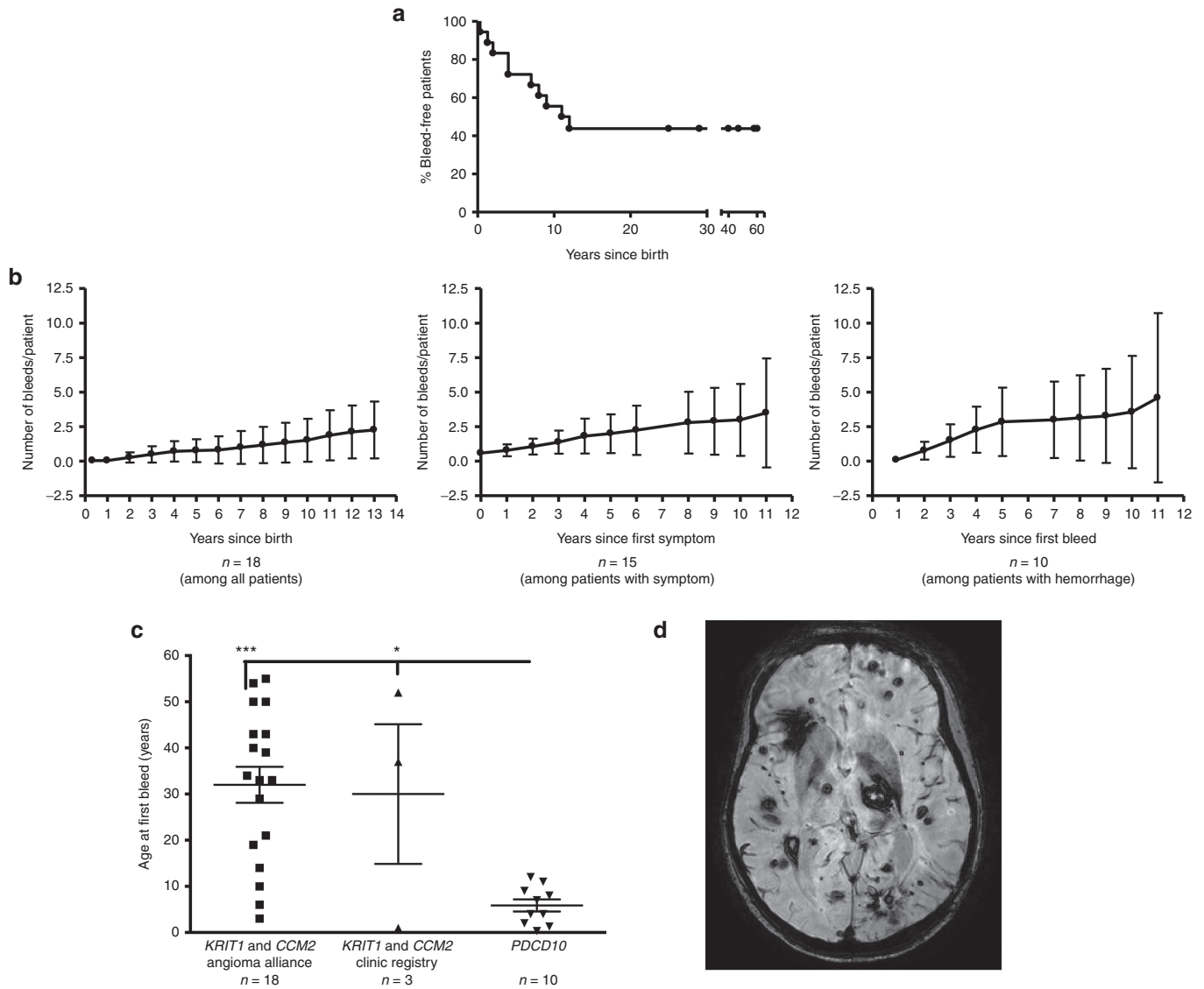


Figure 3 *PDCD10* patients show a more aggressive phenotype. (a) Percentage of bleed-free *PDCD10* patients versus age, showing high bleeding propensity in the first decade of life, leveling off in the teen years. The time of hemorrhage has been established for every adjudicated bleed. (b) Number of bleeds per *PDCD10* patient (mean plotted, with SE bar) versus years since birth, after first-symptom onset, and after first hemorrhage. (c) The age at first bleed is lower in *PDCD10* patients than in *KRIT1* and *CCM2* patients. Data bars are means ± SE. (d) A susceptibility weighted imaging scan showing high lesion burden in a *PDCD10* patient.

those seven cases, two underwent spinal MRI scans, and one harbored a spinal cord CCM lesion. The presence of scoliosis was significantly associated with the rate of recurrent bleed per year after a first documented hemorrhage ($P = 0.001$) and with the rate of bleed per lesion per year after a first bleed ($P = 0.001$). There was no association between the presence of skin lesions or scoliosis and lesion burden, cumulative bleeds per case, the annual bleeding rate, the age at onset of first symptoms, or the age at first bleed.

A brain tumor was found in five cases (28%). Based on MRI features, this had the dural-based appearance of meningioma in two subjects and the intracanalicular nodular appearance of acoustic neuroma in two subjects. An additional subject had a biopsy-proven cerebellar astrocytoma. The presence of brain

tumor was significantly associated with the rate of recurrent bleed per year after a first documented hemorrhage ($P < 0.001$) and with the rate of bleed per lesion per year after a first bleed ($P < 0.001$). However, there was no association of tumor with lesion burden, cumulative bleeds per case, the annual bleeding rate, the age at onset of first symptoms, or the age at first bleed. After Bonferroni correction, scoliosis and brain tumor association with bleeds per year after a first bleed, and with bleeds per lesion per year after the first bleed, were all significant at $P < 0.01$.

Cognitive disability was present in 11 cases (61%), including a learning disorder that was most commonly noted in 8 pediatric cases. Surprisingly, we documented no association between the presence of cognitive disability and lesion burden,

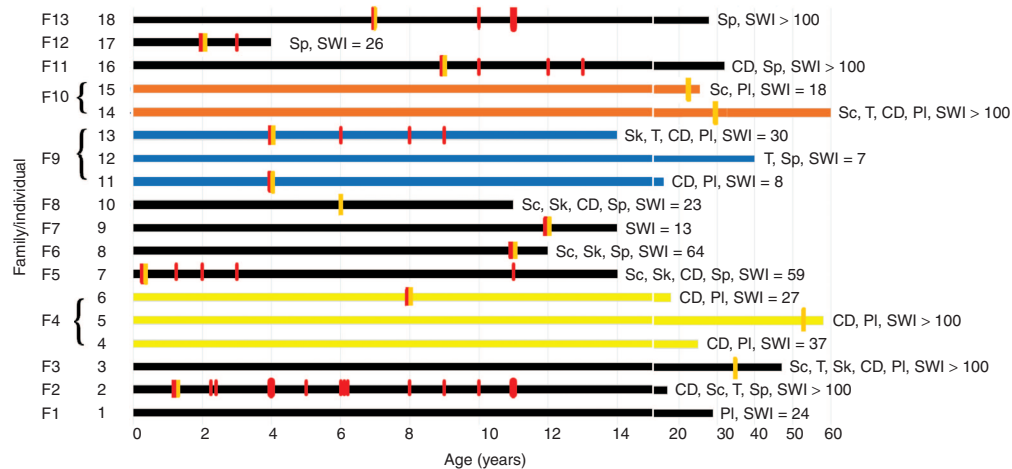


Figure 4 Phenotypic profile of *PDCD10* patients. The cases are grouped by their respective proband (F1–F12). Each subject's lesion burden and clinical associations are indicated. Each symptomatic bleed during the life span of each subject is denoted with a red vertical bar. First symptomatic onset is denoted with a yellow vertical bar. CD, cognitive decline; PDCD, programmed cell death; PI, parental inheritance; Sc, scoliosis; Sk, skin manifestation; Sp, spontaneous mutation; SWI, number of lesions on susceptibility weighted imaging; T, tumor.

cumulative bleeds per case, the annual bleeding rate, the age at onset of first symptoms, or the age at first bleed. Lesion burden may not necessarily result from increased loss of heterozygosity for the *PDCD10* gene. *PDCD10* protein may act through a different mechanism than *KRIT1/CCM2* proteins.^{16–20}

DISCUSSION

Two critical questions were answered in this study, establishing that *PDCD10* mutations result in vascular permeability mediated by ROCK activity and a particularly severe clinical phenotype with previously unappreciated features. Other mechanistic questions remain unanswered, although the current results generate a number of novel hypotheses.

It was shown in recent years that mutations in CCM genes *KRIT1* and *CCM2* result in stress fiber expression and endothelial barrier leak, mediated by ROCK activation.^{15,26} In fact, ROCK³ or broader Rho⁵ inhibition have been advocated as potential therapeutic strategies. Although there is no in vivo confirmation that RhoA is associated with disease manifestations, our data suggest ROCK may be involved in *PDCD10* disease. It has, however, been suggested that *PDCD10* mutations may cause CCM disease via a different mechanism.^{16–20} Vascular permeability and ROCK activity have not been systematically explored as a result of *PDCD10* loss. Brain permeability determined by ROCK activity on MRI in humans with familial CCM is presently being investigated in our laboratory. We now confirm that the expression of stress fibers, endothelial hyperpermeability, and increased ROCK activity occur with loss of *PDCD10*, as we showed previously with the more common *KRIT1* gene.^{3,15} We also demonstrate phenotype rescue in vitro with ROCK inhibition, despite *PDCD10* loss, consistent with a report by Borikova et al.¹⁴

We add other pieces of critical information, including the demonstration of increased ROCK activity in normal background vessels and in CCM lesions in humans and mice

in association with *PDCD10/Pdcd10* loss, characterized by phosphorylated MLC expression and also the more specific ROCK biomarker phosphorylated myosin-binding substrate [Thr⁸⁵³].^{27,28} This and the in vitro results together suggest that ROCK activation plays a similar role in CCM disease associated with *PDCD10* mutations, as with other genotypes. ROCK activity in murine CCM lesions was present regardless of the sensitized background. Mice heterozygous for CCM genes have been shown to manifest hyperpermeability in several vascular beds, including the brain of murine models.^{15,26} For the first time, we document increased brain permeability in the white matter of humans with heterozygous *PDCD10* mutations.

Interesting information was gleaned by comparing lesion burden in *Pdcd10* heterozygous mice and our previously reported heterozygous *Krit1* or *Ccm2* murine models recapitulating the human disease. We previously showed no detectable CCM lesions in *Krit1* or *Ccm2* heterozygous mice, except when they were sensitized with the loss of tumor suppression (*Trp53*) or DNA point mutation repair (*Msh2*) genes,^{21,29} consistent with enhanced lesion genesis as a result of Knudsonian second-hit somatic mutations.^{30,31} In contrast, *Pdcd10* heterozygous mice manifest typical CCM lesions without such sensitization, suggesting a much more penetrant phenotype. Indeed, comparably sensitized heterozygous *Pdcd10* models manifest a tenfold greater lesion burden than other CCM genotypes.

Other studies indicated bleeding earlier in life with this genotype.^{9,11,12} We now provide a systematic correlation with lesion burden, the rate of lesion formation, and hemorrhagic risk. These discoveries would not have been possible without the concerted efforts of Angioma Alliance in facilitating the referral of every known case of *PDCD10* mutation in the United States to a single specialized clinic performing systematic genotyping, phenotypic screening, advanced imaging, and biomarker studies. This represents a model of studying rare diseases, although we acknowledge potential bias despite best currently

available controls. As with mice, we show that patients affected with *PDCD10* mutations have an exceptionally greater lesion burden and more frequent bleeding episodes than other CCM genotypes. They form new small SWI lesions at about twice the rate per year of life and have more clinically relevant lesions on T2-weighted MRI at a rate more than sixfold. Remarkably, each CCM lesion is associated with a very low risk of hemorrhage per year, approximately 0.3%, as was reported with other genotypes.^{6,7,23–25} Hence the bleeding tendency in the *PDCD10* genotype seems to result from a much larger number of lesions, rather than any special lesional vulnerability to hemorrhage. This favors therapeutic targeting of lesion burden or the prevention of lesion development early in life. Patients who have had a first documented symptomatic CCM hemorrhage are often in the first decade of life and are predisposed to recurrent bleeds at a rate of >20% per year, which is higher than any reported with other CCM genotypes.

We document a high frequency of spontaneous mutation in this disease, reflecting in part the very severe phenotype (disability at young age preventing procreation); this is consistent with the previously reported less numerous affected relatives compared with other familial CCM cases.^{2,11,32} Two mutations, c.474+5G>A and c.474+1G>A, were present in three and two unrelated families, respectively. A potential founder effect with these mutations will need to be examined.

The high rates of CCM lesion formation, assuming each lesion represents a separate somatic mutation event, implies that the *PDCD10* locus may be prone to deleterious mutations, possibly representing a mutation hotspot. Many of the second-hit somatic mutations are likely due to loss of heterozygosity generated by mitotic recombination. The location of the three CCM genes on their respective chromosomes in both humans and mice supports a higher frequency of mitotic recombination for the *CCM3/Ccm3* genes. In humans, the *KRIT1/CCM2* gene is located ~32 Mb from the centromere on the q arm of chromosome 7 and the *CCM2* gene is located ~15 Mb from the same centromere on the p arm of chromosome 7, whereas the *PDCD10/CCM3* gene is located ~76 Mb from the centromere on the q arm of chromosome 3 (GRCh38 assembly). In mice, the *Krit1/Ccm1* gene is located ~3.8 Mb from the telocentric centromere on chromosome 5 and the *Ccm2* gene is located ~6.6 Mb from the telocentric centromere on chromosome 11, whereas the *Pdcd10/Ccm3* gene is located ~75 Mb from the telocentric centromere on chromosome 3 (GRCm38 assembly). The larger distance from their respective centromeres to the *CCM3/Ccm3* gene in both species provides the genetic template for an increased opportunity for mitotic recombination, leading to loss of heterozygosity and the initiation of CCM lesion development. Further study of the molecular genetic cause of this phenomenon is needed to explain the exceptional aggressiveness of this disease. There was substantial variability in lesion burden, bleeding, and associated phenotypic features among subjects, among families, and even within respective probands. Factors affecting disease aggressiveness, including

potential genetic and epigenetic modifiers, merit further investigation.

It may be questioned whether each CCM lesion in these patients is the result of a separate and unique somatic mutation. The number of cell divisions and spontaneous mutations necessary during each replication cycle to generate the abundance of lesions many not be possible during the short time frame of lesion genesis in many of these patients' life span. Although somatic biallelic loss of *PDCD10* has been shown in human lesions from familial cases with germline *PDCD10* heterozygosity,³¹ this may not be a requirement for the genesis of every lesion, particularly in the setting of this highly prolific genotype. This will require further investigation, including the sequencing of multiple lesion samples from the same patient or mouse. It is also possible that *PDCD10* may act as a tumor suppressor, inherently sensitizing patients to somatic mutations, and this could also explain the association of tumors with this CCM genotype (see below). This mechanism requires further investigation.

Other phenotypic features are intriguing. An association with skin lesions had been reported primarily with *KRIT1* cases.³³ We now report it with *PDCD10* cases, although the lesions are different (more café-au-lait lesions, for example, rather than keratotic angiomas). Associated meningiomas also have been reported,¹² but herein we document other brain tumors as well. Finally, scoliosis and cognitive impairment in association with this unique cohort are first reported here. Scoliosis may or may not be due to associated spinal lesions; it was not associated with myelopathy, as would be expected with spinal CCMs, and one of two cases with severe scoliosis who underwent spinal MRI had no evidence of spinal CCM lesions. The frequency of disabling cognitive impairment is equally sobering. These novel phenotypic features require further investigation, yet we note no specific relationship of scoliosis or cognitive disability with lesion burden or hemorrhage. This motivates hypotheses about the effect of *PDCD10* loss on skeletal integrity and neurocognitive development and function. These effects might be related to other postulated fundamental roles of *PDCD10* in cell orientation and Golgi assembly,¹⁷ *DLL4*-Notch signaling,¹⁸ and, more recently, neuronal migration.¹³ Herein we note that cognitive impairment in senescence also has been correlated with vascular permeability and ROCK activity.³⁴

In contrast to most patients with CCM with other genotypes, who often live normal lives with infrequent and rarely disabling clinical events, patients with *PDCD10* mutations are frequently devastated by lesion burden and repeated hemorrhages, and these most often start in childhood. Therapeutic strategies need to target children with this disease, perhaps on evidence of a first bleed. At the same time, the high lesion burden in murine models provides an opportunity to detect and optimize therapeutic benefit in the preclinical setting. Fewer subjects would be needed to demonstrate a treatment effect in clinical trials in view of the high rate of lesion genesis in humans and the frequency of clinically significant hemorrhages (particularly rebleeds). ROCK inhibition therapy

is particularly promising and should be explored, along with broader Rho inhibition, documented in pleiotropic effects of statins.³⁵ There has been increasing experience with statin use in childhood, making this therapeutic venue quite realistic if a therapeutic effect and safety of statins are demonstrated in animal models. Brain permeability and other ROCK activity biomarkers³⁶ may help detect treatment effect and calibrate therapy. The association of brain permeability with ROCK activity seen on MRI is being investigated in humans with familial CCMs. Other therapeutic venues with immune modulation^{37,38} and other signaling targets^{4,20,39,40} may realistically be screened given the penetrance of disease in murine models recapitulating the human disease. These may be carefully optimized for clinical trials.

SUPPLEMENTARY MATERIAL

Supplementary material is linked to the online version of the paper at the Genetics in Medicine website <http://www.nature.com/gim>

ACKNOWLEDGMENTS

This work was supported in part by the National Institutes of Health (grant numbers NS077957 to I.A.A. and D.A.M. and 5K01HL092599-04 to R.A.S.), the American Heart Association (grant number 12BGIA9850013 to R.A.S.), and the Bill and Judy Davis Research Fund in Neurovascular Research at the University of Chicago. Recruitment efforts and patient records were provided by CCM3 Action and Angioma Alliance's DNA/Tissue Bank.

DISCLOSURE

The authors declare no conflict of interest.

REFERENCES

1. Maraire JN, Awad IA. Intracranial cavernous malformations: lesion behavior and management strategies. *Neurosurgery* 1995;37:591–605.
2. Bergametti F, Denier C, Labauge P, et al.; Société Française de Neurochirurgie. Mutations within the programmed cell death 10 gene cause cerebral cavernous malformations. *Am J Hum Genet* 2005;76:42–51.
3. McDonald DA, Shi C, Shenkar R, et al. Fasudil decreases lesion burden in a murine model of cerebral cavernous malformation disease. *Stroke* 2012;43:571–574.
4. Maddaluno L, Rudini N, Cuttano R, et al. EndMT contributes to the onset and progression of cerebral cavernous malformations. *Nature* 2013;498:492–496.
5. Li DY, Whitehead KJ. Evaluating strategies for the treatment of cerebral cavernous malformations. *Stroke* 2010;41(10 Suppl):S92–S94.
6. Kondziolka D, Monaco EA 3rd, Lunsford LD. Cavernous malformations and hemorrhage risk. *Prog Neurol Surg* 2013;27:141–146.
7. Al-Shahi Salman R, Hall JM, Horne MA, et al.; Scottish Audit of Intracranial Vascular Malformations (SAIVMs) collaborators. Untreated clinical course of cerebral cavernous malformations: a prospective, population-based cohort study. *Lancet Neurol* 2012;11:217–224.
8. Al-Shahi Salman R, Berg MJ, Morrison L, Awad IA; Angioma Alliance Scientific Advisory Board. Hemorrhage from cavernous malformations of the brain: definition and reporting standards. Angioma Alliance Scientific Advisory Board. *Stroke* 2008;39:3222–3230.
9. Gault J, Sain S, Hu LJ, Awad IA. Spectrum of genotype and clinical manifestations in cerebral cavernous malformations. *Neurosurgery* 2006;59:1278–84; discussion 1284.
10. D'Angelo R, Marini V, Rinaldi C, et al. Mutation analysis of CCM1, CCM2 and CCM3 genes in a cohort of Italian patients with cerebral cavernous malformation. *Brain Pathol* 2011;21:215–224.
11. Denier C, Labauge P, Bergametti F, et al.; Société Française de Neurochirurgie. Genotype-phenotype correlations in cerebral cavernous malformations patients. *Ann Neurol* 2006;60:550–556.
12. Riant F, Bergametti F, Fournier HD, et al. CCM3 Mutations Are Associated with Early-Onset Cerebral Hemorrhage and Multiple Meningiomas. *Mol Syndromol* 2013;4:165–172.
13. Louvi A, Nishimura S, Günel M. Ccm3, a gene associated with cerebral cavernous malformations, is required for neuronal migration. *Development* 2014;141:1404–1415.
14. Borikova AL, Dibble CF, Sciaky N, et al. Rho kinase inhibition rescues the endothelial cell cerebral cavernous malformation phenotype. *J Biol Chem* 2010;285:11760–11764.
15. Stockton RA, Shenkar R, Awad IA, Ginsberg MH. Cerebral cavernous malformations proteins inhibit Rho kinase to stabilize vascular integrity. *J Exp Med* 2010;207:881–896.
16. Chan AC, Drakos SG, Ruiz OE, et al. Mutations in 2 distinct genetic pathways result in cerebral cavernous malformations in mice. *J Clin Invest* 2011;121:1871–1881.
17. Fidalgo M, Fraile M, Pires A, Force T, Pombo C, Zalvide J. CCM3/PDCD10 stabilizes GCKIII proteins to promote Golgi assembly and cell orientation. *J Cell Sci* 2010;123(Pt 8):1274–1284.
18. You C, Sandalcioğlu IE, Dammann P, Felbor U, Sure U, Zhu Y. Loss of CCM3 impairs DLL4-Notch signalling: implication in endothelial angiogenesis and in inherited cerebral cavernous malformations. *J Cell Mol Med* 2013;17:407–418.
19. Yoruk B, Gillers BS, Chi NC, Scott IC. Ccm3 functions in a manner distinct from Ccm1 and Ccm2 in a zebrafish model of CCM vascular disease. *Dev Biol* 2012;362:121–131.
20. Hwang J, Pallas DC. STRIPAK complexes: structure, biological function, and involvement in human diseases. *Int J Biochem Cell Biol* 2014;47:118–148.
21. McDonald DA, Shenkar R, Shi C, et al. A novel mouse model of cerebral cavernous malformations based on the two-hit mutation hypothesis recapitulates the human disease. *Hum Mol Genet* 2011;20:211–222.
22. Ceccarelli DF, Laister RC, Mulligan VK, et al. CCM3/PDCD10 heterodimerizes with germinal center kinase III (GCKIII) proteins using a mechanism analogous to CCM3 homodimerization. *J Biol Chem* 2011;286:25056–25064.
23. Gross BA, Lin N, Du R, Day AL. The natural history of intracranial cavernous malformations. *Neurosurg Focus* 2011;30:E24.
24. Labauge P, Brunereau L, Laberge S, Houtteville JP. Prospective follow-up of 33 asymptomatic patients with familial cerebral cavernous malformations. *Neurology* 2001;57:1825–1828.
25. Zabramski JM, Wascher TM, Spetzler RF, et al. The natural history of familial cavernous malformations: results of an ongoing study. *J Neurosurg* 1994;80:422–432.
26. Whitehead KJ, Chan AC, Navankasattusas S, et al. The cerebral cavernous malformation signaling pathway promotes vascular integrity via Rho GTPases. *Nat Med* 2009;15:177–184.
27. Grassie ME, Moffat LD, Walsh MP, MacDonald JA. The myosin phosphatase targeting protein (MYPT) family: a regulated mechanism for achieving substrate specificity of the catalytic subunit of protein phosphatase type 1δ. *Arch Biochem Biophys* 2011;510:147–159.
28. Murányi A, Derkach D, Erdodi F, Kiss A, Ito M, Hartshorne DJ. Phosphorylation of Thr695 and Thr850 on the myosin phosphatase target subunit: inhibitory effects and occurrence in A7r5 cells. *FEBS Lett* 2005;579:6611–6615.
29. Shenkar R, Venkatasubramanian PN, Wyrwicz AM, et al. Advanced magnetic resonance imaging of cerebral cavernous malformations: part II. Imaging of lesions in murine models. *Neurosurgery* 2008;63:790–7; discussion 797.
30. Gault J, Shenkar R, Recksiek P, Awad IA. Biallelic somatic and germ line CCM1 truncating mutations in a cerebral cavernous malformation lesion. *Stroke* 2005;36:872–874.
31. Akers AL, Johnson E, Steinberg GK, Zabramski JM, Marchuk DA. Biallelic somatic and germline mutations in cerebral cavernous malformations (CCMs): evidence for a two-hit mechanism of CCM pathogenesis. *Hum Mol Genet* 2009;18:919–930.
32. Liquori CL, Berg MJ, Squitieri F, et al. Low frequency of PDCD10 mutations in a panel of CCM3 probands: potential for a fourth CCM locus. *Hum Mutat* 2006;27:118.

33. Sirvente J, Enjolras O, Wassef M, Tournier-Lasserre E, Labauge P. Frequency and phenotypes of cutaneous vascular malformations in a consecutive series of 417 patients with familial cerebral cavernous malformations. *J Eur Acad Dermatol Venereol* 2009;23:1066–1072.
34. Huynh J, Nishimura N, Rana K, et al. Age-related intimal stiffening enhances endothelial permeability and leukocyte transmigration. *Sci Transl Med* 2011;3:112ra122.
35. Zhou Q, Liao JK. Pleiotropic effects of statins. - Basic research and clinical perspectives -. *Circ J* 2010;74:818–826.
36. Liu PY, Liao JK. A method for measuring Rho kinase activity in tissues and cells. *Methods Enzymol* 2008;439:181–189.
37. Zhang Y, Tang W, Zhang H, et al. A network of interactions enables CCM3 and STK24 to coordinate UNC13D-driven vesicle exocytosis in neutrophils. *Dev Cell* 2013;27:215–226.
38. Shi C, Shenkar R, Du H, et al. Immune response in human cerebral cavernous malformations. *Stroke* 2009;40:1659–1665.
39. Fisher OS, Boggon TJ. Signaling pathways and the cerebral cavernous malformations proteins: lessons from structural biology. *Cell Mol Life Sci* 2014;71:1881–1892.
40. Bacigaluppi S, Retta SF, Pileggi S, et al. Genetic and cellular basis of cerebral cavernous malformations: implications for clinical management. *Clin Genet* 2013;83:7–14.